

## TOWARDS UNRAVELLING THE STRUCTURAL DISTRIBUTION OF ULTRA-HIGH-ENERGY COSMIC RAY SOURCES

HAJIME TAKAMI<sup>1</sup> AND KATSUHIKO SATO<sup>1,2</sup>  
takami@utap.phys.s.u-tokyo.ac.jp  
UTAP-587

## ABSTRACT

We investigate the possibility that near future observations of ultra-high-energy cosmic rays (UHECRs) can unveil their local source distribution, which reflects the observed local structures if their origins are astrophysical objects. In order to discuss this possibility, we calculate the arrival distribution of UHE protons taking into account their propagation process in intergalactic space i.e. energy losses and deflections by extragalactic magnetic field (EGMF). For a realistic simulation, we construct and adopt a model of a structured EGMF and UHECR source distribution, which reproduce the local structures actually observed around the Milky Way. The arrival distribution is compared statistically to their source distribution using correlation coefficient. We specially find that UHECRs above  $10^{19.8}$  eV are best indicators to decipher their source distribution within 100 Mpc, and detection of about 500 events on all the sky allows us to unveil the local structure of UHE universe for plausible EGMF strength and the source number density. This number of events can be detected by five years observation by Pierre Auger Observatory.

*Subject headings:* cosmic rays — methods: numerical — IGM: magnetic fields — galaxies: general — large-scale structure of the universe

## 1. INTRODUCTION

The origin of ultra-high-energy cosmic rays (UHECRs) above  $10^{19}$  eV is one of the most intriguing problems in astroparticle physics. Akeno Giant Air Shower Array (AGASA) found statistically significant small-scale clusterings of observed UHECR events with large-scale isotropy (Takeda et al. 1999). The AGASA data set of 57 events above  $4 \times 10^{19}$  eV contains four doublets and one triplet within separation angle of  $2^\circ.5$ , consistent with the experimental angular resolution. The chance probability of observing such multiplets under an isotropic distribution is only about 1% (Hayashida et al. 2000). A combination of the results of many UHECR experiments (including AGASA) also revealed eight doublets and two triplets within  $4^\circ$  on a totally 92 events above  $4 \times 10^{19}$  eV (Uchihori et al. 2000). These multiplets suggest that the origins of UHECRs are point-like sources. For identification of UHECR sources, arrival directions of UHECRs have been observed in detail by High Resolution Fly's Eye (HiRes) and Pierre Auger Observatory (Auger). However, so far, these experiments have reported no significant clustering on the arrival distribution above  $4 \times 10^{19}$  eV (Abbasi et al. 2005a; Mollerach et al. 2007).

Recently, several classes of astrophysical objects in many literature has tested for positional correlations with observed arrival directions of UHECRs. The correlations with BL Lac objects were discussed on the assumptions of smaller deflection angles of UHECRs than the experimental angular resolution and/or neutral primaries (Tinyakov & Tkachev 2001), and in consideration with the deflection by Galactic magnetic field (GMF) (Tinyakov & Tkachev 2002). Gorbunov & Troitsky (2005) considered various classes of powerful extragalactic sources for the correlation study including small corrections of UHECR arrival directions by GMF. Hague et al. (2007) discussed the correlation with nearby active galactic nuclei (AGNs) from RXTE catalog of AGNs. However, these studies have not taken into account UHECR propagation in ex-

tragalactic space. UHECRs above  $8 \times 10^{19}$  eV lose a significant fraction of their energies by photopion production in collision with the cosmic microwave background (CMB) photons during their propagation (Berezinsky & Grigorjeva 1988; Yoshida & Teshima 1993). Thus, UHECRs have *horizons*, which are the maximum distances of their sources that UHECRs can reach the Earth, even if their energies are below  $8 \times 10^{19}$  eV at the Earth. The positional correlations between arrival directions of UHECRs and their source candidates outside the horizons are not significant. (In Hague et al. (2007), only nearby AGNs within the horizons are considered.) In addition to the UHECR horizons, deflections due to extragalactic magnetic field (EGMF) are also important since extragalactic cosmic rays are propagated for a much greater distance than in Galactic space. Propagation process of UHECRs should be considered in such correlation studies.

Yoshiguchi et al. (2003a) investigated the correlation between the arrival distribution of UHECRs and their source distribution taking into account UHECR propagation in intergalactic space with a uniform turbulent EGMF whose strength is 1 nG and coherent length is 1 Mpc. The authors adopted a source distribution with  $10^{-6}$  Mpc<sup>-3</sup> that reproduced the local structures and the AGASA results. They concluded that detection of a few thousand events above  $4 \times 10^{19}$  eV reveal observable correlation with the sources within 100 Mpc.

However, a uniform turbulent field is not realistic EGMF model. Faraday rotation measurements indicate magnetic field strengths at the  $\mu$ G level within inner region ( $\sim$  central Mpc) of galaxy clusters (Kronberg 1994). The evidence for synchrotron emission in numerous galaxy clusters (Giovannini & Feretti 2000) and in a few cases of filaments (Kim et al. 1989; Bagchi et al. 2002) also seems to suggest the presence of magnetic fields with  $0.1 - 1.0 \mu$ G at cosmological structures. Several numerical simulations of large-scale structure formation have confirmed these magnetic structures (Sigl et al. 2003; Dolag et al. 2005).

<sup>1</sup> Department of Physics, School of Science, the University of Tokyo, 7-3-1 Hongo, Bunkyo-ku, Tokyo 113-0033, Japan

<sup>2</sup> Research Center for the Early Universe, School of Science, the University of Tokyo, 7-3-1 Hongo, Bunkyo-ku, Tokyo 113-0033, Japan

Based on these studies, in recent years, we calculated propagation of UHE protons in a structured EGMF which well reproduces the local structures actually observed and simulated their arrival distributions with several normalizations of EGMF strength and several number density of UHECR sources (Takami & Sato 2007). We constrained the source number density to best reproduce the AGASA results. As a result,  $10^{-5} \text{ Mpc}^{-3}$  is the most appropriate number density, which is weakly dependent on EGMF strength. (In rectilinear propagation, similar number density is also obtained in Blasi & de Marco (2005); Kachelriess & Semikoz (2005)) However, this has large uncertainty due to the small number of observed events at present.  $10^{-4} \text{ Mpc}^{-3}$  and  $10^{-6} \text{ Mpc}^{-3}$  are also statistically allowed. Therefore, it is useful to deliberate the correlation between the arrival distribution and the source distribution in the case of these number densities. Note that we revealed in the paper that this uncertainty will be solved by future increase of detected events.

In this study, we calculate the arrival distribution of UHECRs, taking their propagation process into account, and investigate the correlation the arrival distribution and their source distribution in the future. A structured EGMF model and source distribution which can reproduce the local universe actually observed are adopted. The source number density and the EGMF strength are treated as parameters since these have some uncertainty. A goal of this study is that we understand the number of observed events to start to observe the UHECR source distribution by UHECRs and how much the correlation is expected in the future.

Auger has already detected more events above  $10^{19} \text{ eV}$  than those observed by AGASA (Roth et al. 2007). Nevertheless, the event clustering has not observed, as mentioned above. It might be due to EGMF and/or GMF strong enough not to generate the multiplets or statistical fluctuation for small number of observed events at highest energies. In any case, we should predict and discuss how the arrival distribution reflects UHECR source distribution.

Chemical composition of UHECRs is very important for the correlation. If UHECRs are heavier components, magnetic deflections are larger and the correlation is worse. One of observables for study of UHECR composition is the depth of shower maximum,  $X_{\text{max}}$ , which can be measured by fluorescence detectors. Its average value  $\langle X_{\text{max}} \rangle$  is dependent on UHECR composition and energy. HiRes reported that composition of cosmic rays above  $10^{19} \text{ eV}$  is dominated by protons as a result of  $X_{\text{max}}$  measurement (Abbasi et al. 2005b). Recent result by Auger is compatible to the HiRes result within systematic uncertainties (Unger et al. 2007). However, they concluded that the interpretation of  $\langle X_{\text{max}} \rangle$  distribution is ambiguous because of the uncertainties of hadronic interaction at highest energies. Thus, UHECR composition at highest energies is controversial at present. Despite that, in this study, we assume that all UHECRs are protons since composition above  $10^{19} \text{ eV}$  has proton-like feature.

This paper is organized as follows: in section 2 we provide our models of UHECR source distribution and a structured EGMF. In section 3 we explain our calculation method for the arrival distribution with UHECR propagation and statistical method. In section 4, The results of the correlation between the arrival distribution of UHE protons and their source distribution. We summarize this study in section 5.

## 2. SOURCE DISTRIBUTION AND MAGNETIC FIELD

In this section, our models of UHECR source distribution and a structured EGMF are briefly explained. These models are almost the same as those in our previous work. More detailed explanations are written in Takami et al. (2006).

These models are constructed from *Infrared Astronomical Satellite* Point Source Catalogue Redshift Survey (*IRAS* PSCz) catalog of galaxies (Saunders et al. 2000). This is a catalog of flux-limited galaxy survey with large sky coverage ( $\sim 84\%$  of all the sky). Thus, this is appropriate galaxy catalog for the purpose. The selection effects for observation are corrected with luminosity function of the *IRAS* catalog (Takeuchi et al. 2003). We use a set of galaxies after the correction within 100 Mpc (called our sample galaxies below) for construction of our models since small number of galaxies can be observed above 100 Mpc. We adopt  $\Omega_m = 0.3$ ,  $\Omega_\Lambda = 0.7$  and  $H_0 = 71 \text{ km s}^{-1} \text{ Mpc}^{-1}$  as the cosmological parameters.

We assume that subsets of our sample galaxies with specific number densities are UHECR source distributions.  $10^{-4}$ ,  $10^{-5}$  and  $10^{-6} \text{ Mpc}^{-3}$  is considered as the source number density. For the source number densities, we randomly select galaxies from our sample galaxies with probabilities proportional to the absolute luminosity of each galaxy. This method allows constructing source distributions to reflect the cosmic structures. Source distribution above 100 Mpc is assumed to be isotropic and luminosity distribution of galaxies follows the luminosity function. We take the sources until 1 Gpc into account. All sources are assumed to be have the same power for injection of UHE protons.

Our EGMF model also reproduces the local structures actually observed around the Milky way. Several simulations of cosmological structure formation with magnetic field have found that EGMF roughly traces baryon density distribution. (Sigl et al. 2003; Dolag et al. 2005). Our structured EGMF model is constructed with simple assumptions in addition to these results. We constructed matter density distribution from our sample galaxies with a spatial resolution of 1Mpc equal to the correlation length of our EGMF model,  $l_c$ . In each cell, strength of the EGMF is related to matter density,  $\rho$ , as  $|B_{\text{EGMF}}| \propto \rho^{2/3}$  and a turbulent magnetic field with the Kolmogorov spectrum is assumed. The strength of EGMF is normalized to  $B = 0.0, 0.1$  and  $0.4 \mu\text{G}$  at a cell that contains the center of the Virgo Cluster since EGMF strength has some uncertainty as mentioned in section 1. These three normalizations are used for investigation of the spatial correlation between the arrival distribution and the source distribution. Since the EGMF model and the source distribution are constructed from the same galaxy sample, UHECR sources are in the magnetized structure. Note that volume of about 95% has no magnetic field in our EGMF model.

## 3. METHOD OF CALCULATION

### 3.1. Calculation of arrival distribution of UHE protons

Once a source distribution is given, the arrival distribution of UHE protons can be calculated by calculating propagation of protons from their sources to the Earth. In this section, we describe fundamental processes on proton propagation in intergalactic space and our calculation method of the arrival distribution.

UHE protons lose their energies in collision with CMB during their propagation in intergalactic space

(Berezinsky & Grigorieva 1988; Yoshida & Teshima 1993). Higher energy photon backgrounds (e.g. infrared, optical, ultraviolet etc.) are neglected in this study since we treat protons above  $10^{19.6}$  eV. Such protons remain nearly unaffected by the higher energy background photons because of their relatively small number. Protons above  $8 \times 10^{19}$  eV lose their energies by photopion production,  $p + \gamma \rightarrow \pi + X$ . This reaction has large inelasticity ( $\sim 30\%$ ) and relatively short energy-loss length of about a few ten Mpc at  $z = 0$ . Protons with such energies cannot reach the Earth from distant sources. Thus, the photopion production predicts sharply spectral steepening around  $8 \times 10^{19}$  eV, so-called Greisen-Zatsepin-Kuz'min (GZK) steepening (Greisen 1966; Zatsepin & Kuz'min 1966). The GZK effect is essential in considering the correlation with distribution of relatively distant sources. We adopt the energy-loss length which is calculated by simulating the photopion production with the event generator SOPHIA (Mucke et al. 2000). On the other hand, protons below  $8 \times 10^{19}$  eV lose their energies mainly due to Bethe-Heitler pair creation,  $p + \gamma \rightarrow p + e^+ + e^-$ . This has small inelasticity ( $\sim 10^{-3}$ ). We adopt the analytical fit function given by Chodorowski et al. (1992) to calculate the energy-loss rate on isotropic photons. An adiabatic energy loss due to the expanding universe also makes protons lose their energies. The energy-loss rate is written as

$$\frac{dE}{dt} = -\frac{\dot{a}}{a}E - H_0 [\Omega_m(1+z)^3 + \Omega_\Lambda]^{1/2} E. \quad (1)$$

These three energy-loss processes are treated as continuous processes in our calculation.

Trajectories of protons are deflected by EGMF. Protons injected from their sources to the Earth cannot be led into the Earth straightforward. It wastes much CPU time to calculate the propagation of protons which cannot arrive at the Earth in order to construct the arrival distribution. For solving such problem, we suggested a new calculation method of the arrival distribution which is an application of the backtracking propagation (Takami et al. 2006). In this method, protons with the charge of -1 are ejected from the Earth and then we calculate their trajectories in intergalactic space taking into account magnetic deflections and energy-loss(gain) processes. Such trajectories are regarded as those of protons from extragalactic space. We calculate only trajectories of protons which can reach the Earth.

In order to simulate the arrival distribution, 2,500,000 protons (with charges of -1) with  $dN/d\log_{10} E \propto \text{Const.}$  from  $10^{19}$  to  $10^{21}$  eV, are ejected isotropically from the Earth. We calculate their trajectories until their propagation time exceeds the lifetime of Universe or their energies reach  $10^{22}$  eV, which corresponds to the maximum acceleration energy at UHECR sources. For each source distribution, we calculate a factor for a trajectory of  $j$  th particle, which represents the relative probability that the  $j$  th proton reaches the Earth,

$$P_{\text{selec}}(E, j) \propto \sum_i \frac{1}{(1+z_{i,j})d_{i,j}^2} \frac{dN/dE_g(d_{i,j}, E_g^i)}{E^{-1.0}} \frac{dE_g}{dE}. \quad (2)$$

Here  $i$  labels sources on each trajectory, while  $z_{i,j}$  and  $d_{i,j}$  are redshift and distance of such sources.  $E_g^i$  is the energy of a proton at the  $i$  th source, which has the energy  $E$  at the Earth. Thus,  $dN/dE_g(d_{i,j}, E_g^i) \propto E_g^{-2.6}$  is the energy spectrum of UHE protons ejected from a source whose distance is  $d_{i,j}$ .  $dE_g/dE$  represents correction factor for the variation of the shape of the energy spectrum through the propagation.

We randomly select trajectories according to these relative probabilities,  $P_{\text{selec}}$ , so that the number of the selected trajectories is equal to the required event number. The mapping of the

ejected direction of each particle at the Earth is the arrival distribution of UHE protons. If we have to select the same trajectory more than once to adjust the number of selected trajectories, we generate new events whose arrival direction is calculated by adding a normally distributed deviation with zero mean and variance equal to the experimental resolution to the original arrival direction. The experimental resolution is assumed to be  $1^\circ$ .

### 3.2. Statistical Quantities

In order to investigate statistically the similarity between the arrival distribution of UHECRs  $f_e$  and the source distribution  $f_s$ , a correlation coefficient between the two distributions is defined as

$$\Xi(f_e, f_s) \equiv \frac{\rho(f_e, f_s)}{\sqrt{\rho(f_e, f_e)\rho(f_s, f_s)}} \quad (3)$$

where

$$\rho(f_a, f_b) \equiv \sum_{j,k} \frac{f_a(j,k) - \bar{f}_a}{\bar{f}_a} \frac{f_b(j,k) - \bar{f}_b}{\bar{f}_b} \frac{\Delta\Omega(j,k)}{4\pi}. \quad (4)$$

Here subscripts  $j$  and  $k$  distinguish each cell of the sky,  $\Delta\Omega(j,k)$  denotes the solid angle of the  $(j,k)$  cell, and  $\bar{f}_a$  means the average of  $f$  calculated as

$$\bar{f}_a \equiv \sum_{j,k} f_a(j,k) \frac{\Delta\Omega(j,k)}{4\pi}. \quad (5)$$

By definition,  $\Xi$  ranges from -1 to +1. When  $\Xi = +1(-1)$ , the two distributions are exactly the same(opposite). When  $\Xi = 0$ , we cannot find any resemblance between the two distributions. A source at a distance  $d_i$  approximately contributes to arrival cosmic rays with the weight of  $d_i^{-2}$  since all sources are assumed to have the same injection power. Therefore,  $f_s(j,k)$  is calculated as  $\sum_i 1/d_i^2$ , where  $i$  runs over sources in the  $(j,k)$  cell.

## 4. RESULTS

For a given source distribution, we can simulate the arrival distribution of UHE protons using the calculation method explained in the previous section. We investigate the correlation between the arrival distribution and the source distribution, and discuss the possibility to unveil the local structure by UHECRs.

In Fig.1, we demonstrate arrival distributions of UHE protons above  $10^{19.8}$  eV predicted by a specific source distribution with  $10^{-5} \text{ Mpc}^{-3}$  in the galactic coordinate. The EGMF is not included. The source distribution within 100 Mpc is shown on its upper right panel. The radii of circles in this figure are inversely proportional to source distances. The sources within 50 Mpc are shown with bold circles. The number of simulated events are 50 (*upper left*), 200 (*lower left*), 500 (*upper middle*), 1000 (*lower middle*), and 2000 (*lower right*). Note that 50 events on all the sky correspond to the Auger result at present since Auger observes cosmic rays in the southern hemisphere (Roth et al. 2007).

When 200 events are detected, strong event clusterings from nearby sources (within 50 Mpc) can be observed. The distribution of more distant sources are not found yet except for the directions that sources are positionally concentrated. Detection of more than 500 events enables us to find event clusterings in the direction of almost all sources within 100 Mpc. Thus, we can find graphically that detection of about 500 cosmic rays above  $10^{19.8}$  eV makes us unveil nearby source distribution of them.

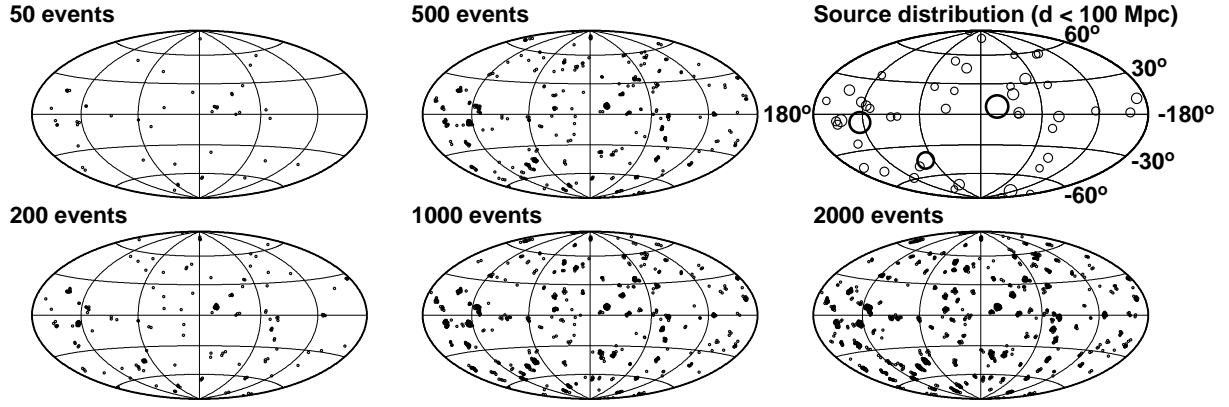


FIG. 1.— The arrival distributions of UHE protons above  $10^{19.8}$  eV predicted by a specific source distribution with  $10^{-5} \text{ Mpc}^{-3}$  (upper right) in the galactic coordinate. The EGMF is not included. The source distribution within 100 Mpc is shown as radii of circles inversely proportional to source distances. The sources within 50 Mpc are shown with bold circles. The simulated number of events are 50 (upper left), 200 (lower left), 500 (upper middle), 1000 (lower middle), and 2000 (lower right).

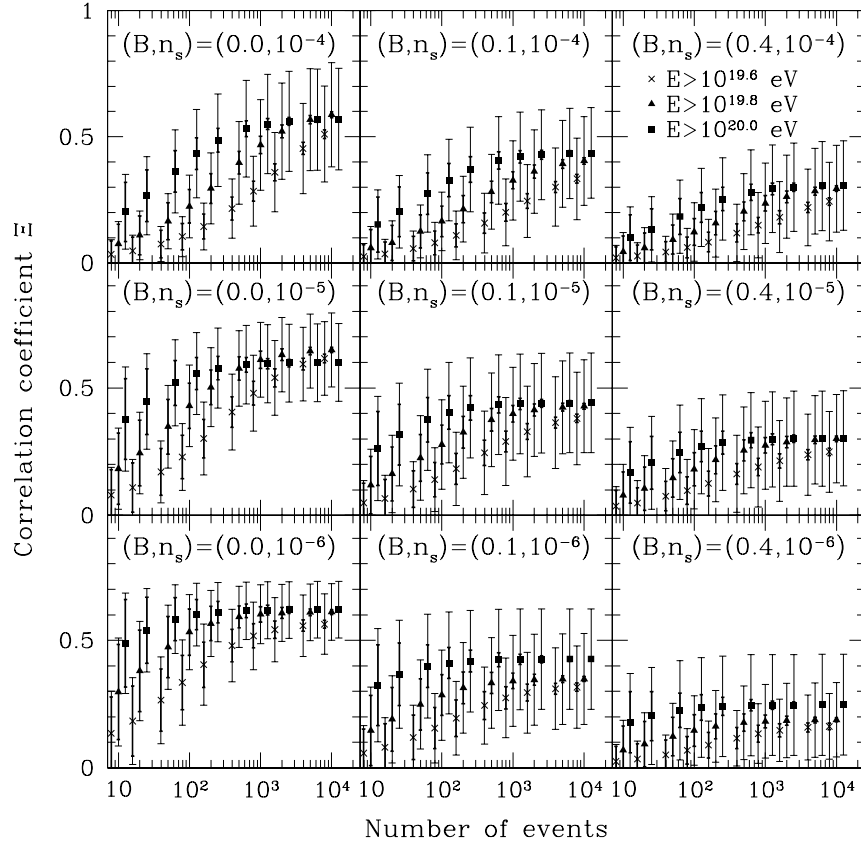


FIG. 2.— Correlation coefficients between the arrival distribution of UHE protons above  $10^{19.6}$  (crosses),  $10^{19.8}$  (triangles) and  $10^{20.0}$  eV (squares), and their source distribution within 100 Mpc for several EGMF strengths and the number densities of UHECR sources as a function of expected number of cosmic rays on all the sky. The size of the cell for the calculation of the correlation coefficients is chosen to be  $2^\circ \times 2^\circ$ . The three marks on the same number of events are a little shifted horizontally for visibility. Units of  $B$ , normalization factor of the EGMF strength, and  $n_s$ , the source number density, is  $\mu\text{G}$  and  $\text{Mpc}^{-3}$  respectively. The short (thick) error bars represent the fluctuations due to the finite number of observed events and the long (thin) error bars are total errors including the cosmic variance.

We should discuss statistically (not graphically) the probability that future observations can unveil UHECR source distribution. Fig.2 shows predicted correlation coefficients between the arrival distribution of UHE protons and their source distribution within 100 Mpc for several EGMF strengths and source number densities as a function of expected number of cosmic ray events. The size of the cell for the calculation of the correlation coefficients is chosen to be  $2^\circ \times 2^\circ$  since angular resolution of UHECR experiments,  $1^\circ$ , is taken into account in simulating the arrival directions. The numbers of events that we calculate the correlation coefficients are 10, 20, 50, 100, 200, 500, 1000, 2000, 5000, 10000 on all the sky for  $E > 10^{19.6}$  (crosses),  $E > 10^{19.8}$  (triangles), and  $E > 10^{20.0}$  eV (squares). The three marks on the same number of events are slightly shifted horizontally for visibility. The EGMF strengths,  $B$ , and the source number densities,  $n_s$ , which are adopted for the simulation are represented on each panel. There are two errors. The thick (short) error bars show the statistical error, i.e., the fluctuations due to the finite number of observed events, averaged over 100 realizations of the source distribution for a given source number density. The random event selection to estimate the fluctuations is performed 100 times for each source distribution. On the other hand, the thin (long) error bars represent the total error, i.e., the statistical error plus the cosmic variance. The latter error bars also include the variation between different realizations of source distributions. Note that statistical errors on an observation are estimated as the thick error bars since only a source distribution is true in the Universe.

First, we deliberate the correlation in the case of no magnetic field. A lot of features of the correlation coefficients common to finite EGMF cases are found in this simplest case. The three left panels show the correlation coefficients in the case of no EGMF. When the numbers of observed events increase, the correlation coefficients start to converge, and the final values can be estimated. The statistical errors (thick error bars) decrease. The cosmic variance remains at large number of events since it is uncertainty to originate from different source distributions. Note that a source distribution used in Fig.1 predicts correlation coefficients similar to the averages of those in the middle left panel of Fig.2. The correlation coefficient cannot converge on 1.0 in spite of rectilinear propagation due to the finite angular resolution, the energy loss processes, and also because cosmic rays do not always come from sources within 100 Mpc. Since UHE protons from more distant source needs the higher energy at the source in order to reach the Earth with the same energies, such source contributes to arrival cosmic rays smaller than nearer source even if a factor of  $d_i^{-2}$  is taken into account. In other words, the arrival distribution of many cosmic rays is only approximately the same spatial pattern as their source distribution weighted by  $d_i^{-2}$ .

We focus on the behaviors of averages of the correlation coefficients on each panel. The correlation coefficients with protons above  $10^{20}$  eV predict larger values than those with lower energies at the small number of observed events. As the number of detected events increases, the coefficients with highest energies converge on the smaller values than those with lower energies. The reason is GZK mechanism. UHE protons above  $10^{20}$  eV can come from sources only within the GZK sphere ( $\sim 50$  Mpc). On the other hand, protons with lower energies can arrive at the Earth outside 100 Mpc. Thus, the correlations are better at the small number of events. The difference between the correlation coefficients with protons above  $4 \times 10^{19}$  eV and

those above  $10^{20}$  eV is statistically significant at  $1\sigma$  level since strengths of errors on observation are estimated as the thick error bars. Since the radius of the GZK sphere is less than 100 Mpc, there are sources within 100 Mpc which cannot be traced by cosmic rays above  $10^{20}$  eV. Thus, as the number of observed events increases, the correlation coefficients with such highest energy protons converge on a little smaller values than those with lower energy protons. The correlations of protons with  $E > 10^{19.8}$  eV are better than those with  $E > 10^{19.6}$  eV, because lower energy protons can reach the Earth from more distant sources.

Next, we investigate the correlation including EGMF. The three middle panels and the three right panels of Fig.2 show the correlation coefficients in the case of  $B = 0.1$  and  $0.4 \mu\text{G}$  respectively. The EGMF diffuses trajectories of UHECRs during their propagation and obscures their arrival directions (Takami et al. 2006). Therefore, stronger EGMF predicts weaker correlation in any source number density. Compared to the correlation coefficient in the case of no EGMF, that of protons with the lower energy threshold is worse since lower energy protons are deflected by EGMF more largely. Protons with  $E > 10^{19.6}$ ,  $10^{19.8}$  eV predicts smaller correlation than those above  $10^{20}$  eV.

The number of events that the correlation coefficients start to converge is weakly dependent on the EGMF strength and depends on the source number density. In the case of  $10^{-6}$  Mpc $^{-3}$ , such numbers of events are about 1,000, 200, and 50 for  $E > 10^{19.6}$ ,  $10^{19.8}$  and  $10^{20}$  eV respectively. At larger number densities, such numbers increase. In the case of  $10^{-5}$  ( $10^{-4}$ ) Mpc $^{-3}$ , these numbers are about 5,000 ( $> 10000$ ), 500 (5000), and 100 (500) for  $E > 10^{19.6}$ ,  $10^{19.8}$  and  $10^{20}$  eV respectively. Detection of such number of events enables us to unveil UHECR source distribution at visible level by UHE protons, which concerned with the final value of the correlation coefficients. Both cosmic rays above  $10^{19.8}$  eV and those above  $10^{20}$  eV are good indicators for unravelling the source distribution since their correlation values converge to nearly equal values for  $10^{-4}$  and  $10^{-5}$  Mpc $^{-3}$ . However, the detected number of cosmic rays above  $10^{19.8}$  eV reaches the number that the correlation coefficient starts to converge in shorter observing period than that of cosmic rays above  $10^{20}$  eV since cosmic rays above  $10^{20}$  eV are almost not detected in the presence of the GZK steepening. Note that our source model predicts the GZK steepening. Thus, UHE protons above  $10^{19.8}$  eV are best indicators to unveil the source distribution within 100 Mpc. Note that ground based detectors such as Auger and Telescope Array (TA) (Fukushima et al. 2007) can observe only about half hemisphere, so only half of such numbers are observed.

Fig.3 is the simulation of the arrival distribution of UHE protons above  $10^{19.8}$  eV in the case of  $B = 0.1$  and  $0.4 \mu\text{G}$ . The source distribution is the same one in Fig.1. In Fig.1 and 3, the arrival distributions with 200 protons (less than 500 events, which is the number that the correlation coefficients start to converge) include several number of event clusterings. Compared to the three cases of the EGMF strength, the arrival directions of protons are diffused by EGMF. We can also find event clusterings in the directions of nearby sources or source clusterings. Such event clusterings are not lost by a structured EGMF although their angular scales are spread. At 500 event detection, the event clusterings increase and the local structure of the universe appears.

The larger size of the cell for the calculation of the corre-

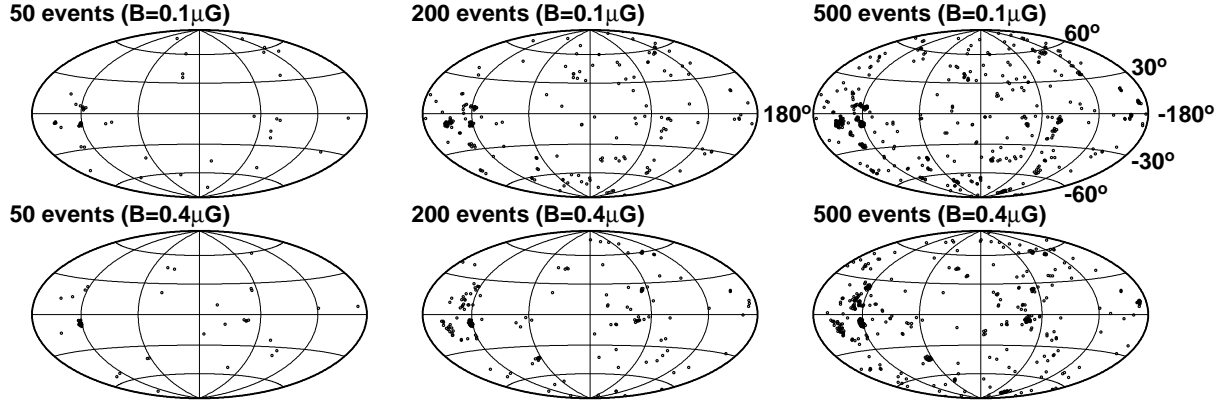


FIG. 3.— The arrival distributions of UHE protons above  $10^{19.8}$  eV predicted by the same source distribution used in Fig. 2. The upper panels show those taking into account propagation in the EGMF with  $B = 0.1 \mu\text{G}$  and the lower panels are the same, but  $B = 0.4 \mu\text{G}$ .

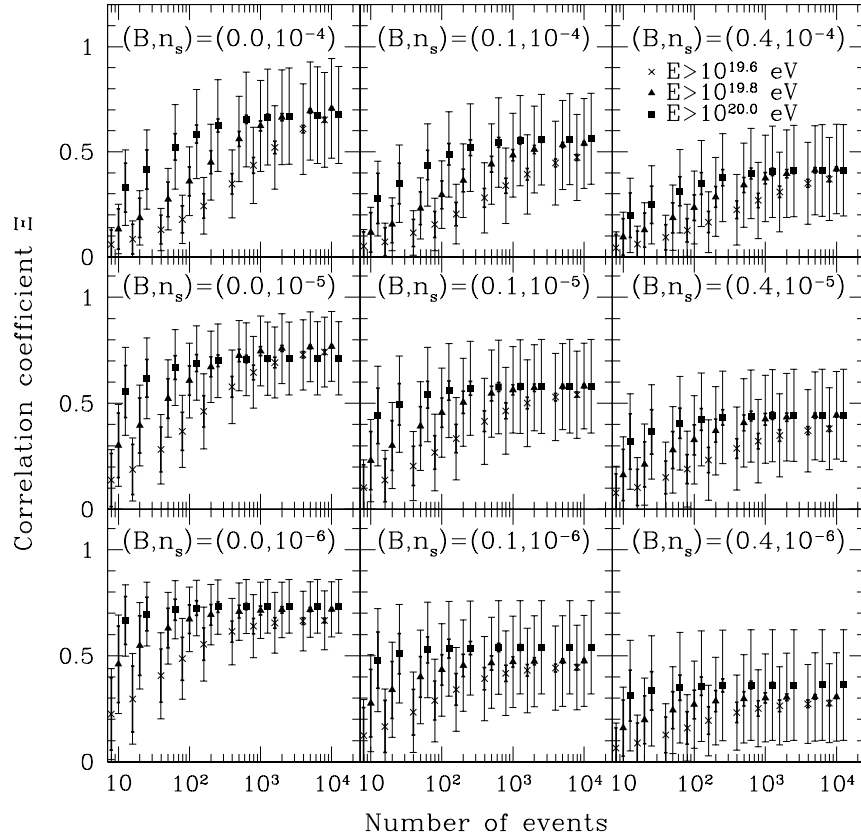


FIG. 4.— Same as Fig. 2, but for  $4^\circ \times 4^\circ$ .

lation coefficients is expected to lead to larger correlation coefficients since EGMF obscures UHECR arrival directions as mentioned above. Fig.4 shows the same figure, but the size of the cell is chosen to be  $4^\circ \times 4^\circ$ . The correlation coefficients are larger than those in Fig.2 on all panels. These increase even in the case of  $B = 0.0\mu\text{G}$  since a part of arrival cosmic rays from a source is distributed in a small scale, but larger than  $2^\circ$  due to finite angular resolution of UHECR experiments. The values of the coefficients are slightly not increase even if the size of the cell is larger than  $4^\circ \times 4^\circ$ . In this figure, we find that the numbers of events starting the convergence of the correlation coefficients are almost unchanged.

## 5. CONCLUSION

In this paper, we calculated the arrival distribution of UHE protons taking into account energy losses and deflections by EGMF during propagation in intergalactic space in order to investigate the possibility that future observations of UHECRs can unveil the local structure of UHE universe. In order to reproduce a realistic situation, we adopted a structured EGMF model and source distributions which reproduce the observed local structures. The arrival distribution of UHE protons was compared statistically to their source distribution using the correlation coefficients. As the number of observed events increases, the correlation coefficient increases and converges to some value which represents the ability to unveil the source distribution by UHE protons, i.e. charged particles. Thus, the number of events that the correlation coefficient starts to converge is an important number for UHECR observations. In other words, detection of such number of events allows us to unravel UHECR source distribution. We found that UHECRs

above  $10^{19.8}\text{eV}$  are best indicators to decipher their source distribution within 100 Mpc from discussion based on the final values of the correlation coefficients and GZK mechanism, and 5000, 500, and 200 event detections above  $10^{19.8}\text{eV}$  on all the sky can unveil their source distribution for the source number densities of  $10^{-4}$ ,  $10^{-5}$ , and  $10^{-6}\text{Mpc}^{-3}$  respectively. Note that ground based detectors observe only about half hemisphere, so only half of such numbers are requested.

In this study, we took only EGMF into account as magnetic field, i.e., neglected GMF. GMF deflects trajectories of UHE protons efficiently by its regular components, which consist in spiral and dipole components (Alvarez-Muniz et al. 2002; Yoshiguchi et al. 2003b). A turbulent component of GMF very weakly change the arrival directions of UHE protons (Yoshiguchi et al. 2004). The deflection angles of UHECR protons are a few degree at around  $10^{20}\text{eV}$  except for the direction of Galactic Center. Such deflection disturbs the spatial pattern of UHECR arrival distribution at a few degree scale. The effect of GMF is one of our future investigations.

A lot of inquiries on UHECR source number density result in around  $10^{-5}\text{Mpc}^{-3}$  on ground of the AGASA results as introduced in section 1. If this number density is true, five year observation by Auger and future observation by TA and Extreme Universe Space Observatory (Ebisuzaki et al. 2007) will reveal the distribution of nearby UHECR sources. The dawn of the UHE particle astronomy is just around the corner.

The work of H.T. is supported by Grants-in-Aid for JSPS Fellows. The work of K.S. is supported by Grants-in-Aid for Scientific Research provided by the Ministry of Education, Science and Culture of Japan through Research Grants S19104006.

## REFERENCES

- Abbasi, R.U., et al. 2005a, *ApJ*, 623, 164  
 Abbasi, R.U., et al. 2005b, *ApJ*, 622, 910  
 Alvarez-Muniz, J., Engel, R., & Stanev, T. 2002, *ApJ*, 572, 185  
 Bagchi, J., et al. 2002, *New Astron.*, 7, 249  
 Blasi, P., & de Marco, D. 2004, *Astropart. Phys.*, 20, 559  
 Berezhinsky, V., & Grigorieva, S.I. 1988, *A&A*, 199, 1  
 Chodorowski, M. J., Żdziarski, A. A., & Sikora, M. 1992, *ApJ*, 400, 181  
 Dolag, K., et al. 2005, *J. Cosmology Astropart. Phys.*, 0501, 009  
 Ebisuzaki et al. 2007, *Proc. 30th Int. Cosmic Ray Conf. (Merida)*, #831  
 Fukushima et al. 2007, *Proc. 30th Int. Cosmic Ray Conf. (Merida)*, #955  
 Giovannini, G., & Feretti, L. 2000, *New Astron.*, 5, 335  
 Gorbunov, D.S., & Troitsky, S.V. 2005, *Astropart. Phys.*, 23, 175  
 Greisen, K. 1966, *Phys. Rev. Lett.*, 16, 74  
 Hayashida, N., et al. 2000, *AJ*, 120, 2190  
 Hague, J.D., et al. 2007, *Astropart. Phys.*, 27, 134  
 Kachelriess, M., & Semikoz, D. 2005, *Astropart. Phys.*, 23, 486  
 Kim, K.T., et al. 1989, *Nature*, 341, 720  
 Kronberg, P.P. 1994, *Rep. Prog. Phys.*, 57, 325  
 Mollerach, S., [Pierre Auger Collaboration] 2007, *preprint arXiv:0706.1749*  
 Mucke, A., et al. 2000, *Comput. Phys. Commun.*, 124, 290  
 Roth, M., [Pierre Auger Collaboration] 2007, *preprint arXiv:0706.2096*  
 Saunders, W., et al. 2000, *MNRAS*, 317, 55  
 Sigl, G., Miniati, F., & Ensslin, T.A. 2003, *Phys. Rev. D*, 68, 043002  
 Takami, H., Yoshiguchi, H., & Sato, K. 2006, *ApJ*, 639, 803 (erratum 653, 1584[2006])  
 Takami, H., & Sato, K. 2007, *in preperation*  
 Takeda, M., et al. 1999, *ApJ*, 522, 225  
 Takeuchi, T. T., Yoshikawa, K., & Ishii, T.T. 2003, *ApJ*, 587, L89 (erratum 606, L171[2004])  
 Tinyakov, P.G., & Tkachev, I.I. 2001, *JETP Lett.*, 74, 445  
 Tinyakov, P.G., & Tkachev, I.I. 2002, *Astropart. Phys.*, 18, 165  
 Uchihori, Y., et al. 2000, *Astropart. Phys.*, 13, 151  
 Unger, M., [Pierre Auger Collaboration] 2007, *preprint arXiv: 0706.1495*  
 Yoshiguchi, H., Nagataki, S., & Sato, K. 2003, *ApJ*, 592, 311  
 Yoshiguchi, H., Nagataki, S., & Sato, K. 2003, *ApJ*, 596, 1044  
 Yoshiguchi, H., Nagataki, S., & Sato, K. 2004, *ApJ*, 607, 840  
 Yoshida, S., & Teshima, M. 1993, *Prog. Theor. Phys.*, 89, 833  
 Zatsepin G.T., & Kuz'min V.A. 1966, *JETP Lett.*, 4, 78